

# SEISMIC DEFORMATION ANALYSIS OF EARTH DAMS

V.G.GHAHRAMAN<sup>1</sup>

M.K.YEGIAN<sup>2</sup>

## I. INTRODUCTION

This paper describes a procedure for the Seismic Deformation Analysis of earth dams. Based on actual earthquake records, an analytical model was developed for calculation of permanent deformation of earth dams. The method involves the integration of the seismological and geotechnical inputs in a consistent manner to yield the seismically induced permanent deformation of the dam. Then, the proposed deformation model is compared with the deformation of the triangular, sinusoidal, and rectangular pulses, as well as the data by Makdisi and Seed (1978).

## II. SEISMIC DEFORMATION ANALYSIS (SDA)

The objective of a Seismic Deformation Analysis is to provide the estimate of permanent deformation of an earth dam upon the occurrence of a specified level of seismic loading. Damage to or failure of an earth dam can occur during or shortly after a seismic event. During shaking, a section of the dam will experience substantial permanent deformation if the earthquake induced shear stresses exceed the shearing resistance of the embankment or foundation materials. The dam may suffer limited damage or may experience total failure due to overtopping, if the available freeboard is lost. In this paper only the deformations that occur during the earthquake have been considered for analysis. However, study should also be extended to the deformations that occur after the shaking stops.

---

<sup>1</sup> Doctoral Candidate, Dept. of Civil Eng'g, Northeastern University, Boston, Mass., U.S.A..

<sup>2</sup> Professor and Chairman, Dept. of Civil Eng'g, Northeastern University, Boston, Mass., U.S.A..

## II-1 Earthquake-Induced Permanent Deformations

Earthquake-induced permanent deformations of an earth dam can be estimated by a number of approaches, varying in their degree of sophistication. On the one hand, Newmark (1965) and Makdisi and Seed (1978) developed empirical charts to estimate the permanent deformation. On the other hand, two dimensional finite element analysis combined with cyclic simple shear or triaxial compression test results on undisturbed or reconstituted soil samples have also been used to evaluate the strain potentials and permanent deformations within a dam subjected to seismic excitations (2, 4, 7, 8, 11, 12, 13, 14, 15, 16, 18).

In the development of the Seismic Deformation Analysis procedures described in this paper, an analytical model was developed for the calculation of permanent deformation that satisfies the following criteria:

- (a) The permanent deformation model is simple enough to be conveniently applied in design practice, yet accounts for all the pertinent seismic and material parameters.
- (b) The model parameters can be evaluated in simple approximate ways or using rigorous sophisticated procedures as dictated by need.
- (c) The model, with some modifications, will allow for the application of probability theory to estimate the likelihood of the permanent deformation exceeding specified values.

The following section describes the procedure that was developed to estimate permanent deformations.

## II-2 Procedure for Calculating Permanent Deformations

Calculation of earthquake-induced permanent deformations can be made using Newmark's sliding block model shown in Figure 1. In this approach, a rigid-plastic response is assumed, such that if the acceleration of the block representing a section of an earth dam exceeds a limiting yield level,  $K_y$ , then a relative displacement,  $D_r$ , will be initiated representing a permanent deformation of the dam section. An illustration of the motions of the block and the base for a triangular base excitation is also presented in Figure 1. Mathematical expressions for  $D_r$  given triangular, sinusoidal, and rectangular base excitations were derived (6). Based on these derivations for  $D_r$ , the following observations are made:

(a) The expression for  $D_r$  is of the form:

$$D_r = f\left(\frac{K_y}{K_a}\right) N_{eq} K_a T^2 \quad (1)$$

in which  $f(\ )$  is a function that depends on the type of base motion considered,  $K_y$  is the yield acceleration,  $K_a$  is the peak acceleration of the base,  $T$  is the period of the motion, and  $N_{eq}$  is the number of uniform cycles of the base motion.

(b) The permanent deformation,  $D_r$ , can be normalized with respect to the peak acceleration of the base,  $K_a$ , and the square of the period of the base motion,  $T$ , and the number of the uniform cycles,  $N_{eq}$ , as shown in Equation 2.

$$D_n = \frac{D_r}{K_a N_{eq} T^2} = f\left(\frac{K_y}{K_a}\right) \quad (2)$$

where  $D_n$  is referred to as the normalized permanent deformation and is a function of only  $K_y$ ,  $K_a$ , and type of base motion.

Figure 2 also shows plots of  $D_n$  versus  $K_y/K_a$  for each of the three simple base motions considered, i.e. triangular, sinusoidal, and rectangular. It is clear that the shape of the base motion has an important effect on the permanent deformation, especially if  $K_y/K_a$  is nearly 1.0. Recognizing that none of these motions properly depict the random nature of earthquake-induced ground motions, a more realistic determination

of the function  $f(\cdot)$  of Equation 2 was made by considering actual earthquake records. The permanent deformations computed by Franklin and Chang (1977) using 86 actual recorded acceleration time-histories for the base motion in Newmark's sliding-block analysis were summarized (6). In this paper, their computed permanent deformations were normalized according to Equation 2 in order to establish the functional relationship between  $D_n$  and  $K_y/K_a$ .

A plot of the normalized permanent deformations,  $D_n$ , for each of the three ratios of  $K_y/K_a$  values of 0.02, 0.1, and 0.5, considered by Franklin & Chang (1977), is shown in Figure 3. The peak ground accelerations and the predominant periods for these records were obtained from Chang (1978), and their number of equivalent cycles of ground motion from Asturias & Dobry (1982). The determination of the permanent deformation function using these data is described in the following section.

### II-3 Function for Permanent Deformations

To establish the function  $f(\cdot)$  of Equation 2 based on actual earthquake records a third degree polynomial was fitted to the data plotted in Figure 3, using Lagrange interpolation. The polynomial was fitted through the median values of the plotted data points at  $K_y/K_a = 0.02, 0.1, \text{ and } 0.5$  thus, deemphasizing the effect of the few extreme points at the high end, which are orders of magnitude different than the next highest values. In addition,  $D_n$  was assigned a very small value ( $10^{-5}$ ) at  $K_y/K_a = 1.0$ , in order to account for the fact that the displacement should be zero if  $K_y/K_a = 1.0$ . This value was selected in order to obtain for  $f(\cdot)$  in the range of  $0.5 < K_y/K_a < 1.0$  (where data is lacking) a shape consistent with that of the triangular base motion which appears to be more representative of actual earthquake motion than the sinusoidal or the rectangular base motions (see Figure 5). The resulting polynomial curve is shown in Figure 4, and its mathematical expression is:

$$\begin{aligned} \log D_n &= \log f(K_y/K_a) \\ &= g(K_y/K_a) = 0.22 - 10.12(K_y/K_a) + 16.38(K_y/K_a)^2 - 11.48(K_y/K_a)^3 \quad (3) \end{aligned}$$

where 
$$D_n = \frac{D_r}{K_a N_{eq} T^2} = f\left(\frac{K_y}{K_a}\right)$$

#### II-4 Comparison of the Proposed Function With Other Models

In Figure 5, the polynomial curve proposed for the calculation of seismically induced permanent deformations is compared with the deformation of the triangular, sinusoidal, and rectangular pulses. For  $K_y/K_a < 0.1$  these simple base motions yield significantly lower values of  $D_n$  than obtained based on Franklin and Chang's integration of recorded time histories. Conversely, for  $K_y/K_a > 0.1$ , the sine and rectangular base motions yield significantly higher values of  $D_n$ . For  $K_y/K_a > 0.1$  the assumption of a triangular pulse yields deformations that are generally in agreement with Franklin and Chang's data and thus with the established function for permanent deformations.

Figure 5 also shows values of  $D_n$  estimated based on the results of Makdisi and Seed (1978) for Richter magnitudes of 6.5, 7.5, and 8.25. These values of  $D_n$  were obtained by normalizing the displacements computed by Makdisi and Seed with respect to the peak acceleration of the potential sliding mass of the dam,  $K_a$ , the square of the first mode fundamental period of the dam,  $T$ , and the number of equivalent uniform cycles of the ground motion,  $N_{eq}$ . The data thus obtained plot slightly below the proposed function. This could be explained by the fact that the periods of the dams used to normalize Makdisi and Seed data are larger than the period of the motion of the dam. Nevertheless, it is noted that Makdisi and Seed data plot within the range of data presented by Franklin and Chang.

### III. SUMMARY AND CONCLUSION

A procedure was described for the Seismic Deformation Analysis of earth dams. Based on actual earthquake records, an analytical model was developed for calculation of permanent deformation of earth dams. The method involves the

integration of the seismological and geotechnical inputs in a consistent manner to yield the seismically induced permanent deformation of the dam. Then, the proposed deformation model is compared with the deformation of the triangular, sinusoidal, and rectangular pulses, as well as the data by Makdisi and Seed (1978). The model, with some modifications, will allow incorporation of uncertainties in the parameters for more realistic assessment of the permanent deformation of earth dams (17,19).

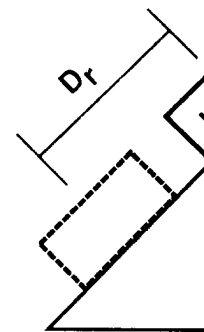
#### **IV. ACKNOWLEDGEMENTS**

The research described in this paper was sponsored by the National Science Foundation through Grant No. DFR-84-12124 for research on Integrated Seismic Risk Analysis for Earth Dams. The writers greatly acknowledge this support.

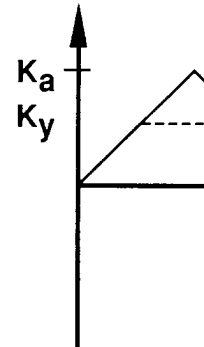
## REFERENCES

1. Asturias R.W., Dobry R., "The Equivalent Number of Cycles of Recorded Accelerograms for Soil Liquefaction Studies," Report No. CE-82-5, Dept of Civil Eng'g, R.P.I., Troy, New York, April, 1982.
2. Chaney R.C., "Earthquake Induced Deformations in Earth Dams," Proc. of the 2nd U.S. Nat. Conf. on Earthq. Eng'g, Stanford Univ., Calif., 1979, pp. 633-642.
3. Chang F.K., "Catalogue of Strong Motion Earthquake Records, Volume 1, Western United States, 1933-1971," State of the Art for Assessing Earthquake Hazards in the United States, Report 9, U.S. Army Engineer Waterways Experiment Station, Misc. Paper No. S-73-1, April, 1978.
4. Elgamal A.W., Abdel-Ghaffar A.M., Prevost J.H., "2-D Elastoplastic Seismic Shear Response of Earth Dams: Application," J. Geotech. Eng'g, ASCE, Vol. 113, No. 5, May, 1987, pp. 702-719.
5. Franklin A.G., Chang F.K., "Permanent Displacements of Earth Embankments by Newmark Sliding Block Analysis," Earthquake Resistance of Earth and Rock-Fill Dams, Report 5, U.S. Army Engineer Waterways Experiment Station, Misc. Paper No. S-71-17, Nov., 1977.
6. Ghahraman V.G., "Seismic Deformation Analysis of Earth Dams," Masters Report submitted to the Dept. of Civil Eng'g at Northeastern Univ. Boston, Mass., Sept. 1988.
7. Lee K.L., "Seismic Permanent Deformations in Earth Dams," Report No. UCLA-ENG-7497, School of Eng'g and Applied Sciences, U.C.L.A., Calif., Dec., 1974.
8. Lee K.L., "Seismic Stability Analysis of Hawkins Hydraulic Fill Dam," J. Geotech. Eng'g, ASCE, Vol. 103, No. GT6, June, 1977, pp. 627-644.
9. Makdisi F.I., Seed H.B., "Simplified Procedure for Estimating Dam and Embankment Earthquake-Induced Deformations," J. Geotech. Eng'g, ASCE, Vol. 104, No. GT7, July, 1978, pp. 849-867.

10. Newmark N.M., "Effects of Earthquakes on Dams and Embankments," *Geotechnique*, Vol. 15, No. 2, June, 1965, pp. 139-160.
11. Paskalov T.A., "Permanent Displacement Estimation on Embankment Dams Due to Earthquake Excitations," Proc. of the 8th World Conf. on Earthq. Eng'g, San Francisco, 1984, pp. 327-334.
12. Prevost J.H., Abdel-Ghaffar A.M., Lacy S.J., "Non-Linear Dynamic Analysis of an Earth Dam," *J. Geotech. Eng'g, ASCE*, Vol. 111, No. 7, July, 1985, pp. 882-897.
13. Resendiz D., Romo M.P., "Analysis of Embankment Deformations," Proc. of Specialty Conf. on Perf. of Earth and Earth-Supported Structures, ASCE, Purdue Univ., Indiana, June, 1972, Vol. I, Part I, pp. 817-776.
14. Seed H.B., Lee K.L., Idriss I.M., Makdisi F.I., "The Slides in the San Fernando Dams During the Earthquake of February 9, 1971," *J. Geotech. Eng'g, ASCE*, Vol. 101, No. GT7, July, 1975, pp. 651-688.
15. Seed H.B., Idriss I.M., Lee K.L., Makdisi F.I., "Dynamic Analysis of the Slide in the Lower San Fernando Dam During the Earthquake of February 9, 1971," *J. Geotech. Eng'g, ASCE*, Vol. 101, No. GT9, Sept., 1975, pp. 889-911.
16. Serff N., Seed H.B., Makdisi F.I., Chang C.Y., "Earthquake Induced Deformation of Earth Dams," Report No. EERC 76-4, Univ. of Calif., Berkeley, Sept., 1976.
17. Sewell R T., "Simplified Seismic Reliability Analysis of Earth Dams," Ph.D. Dissertation, Dept. of Civil Eng'g, Stanford Univ., Calif., Sept., 1984.
18. Taniguchi E., Whitman R.V., Marr W.A., "Prediction of Earthquake-Induced Deformation of Earth Dams," *Soils and Foundations*, Vol. 23, No. 4, Dec., 1983, pp. 126-132.
19. Yegian M.K., Marciano E.A., Ghahraman V.G., "Integrated Seismic Risk Analysis For Earth Dams," Report No. CE-88-12. Dept. of Civil Eng'g, Northeastern Univ., Boston, Mass., Dec. 1988.



support acceleration



displacement

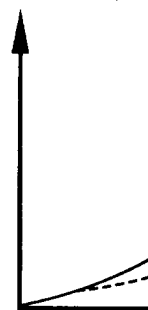


FIGURE 1 SLIDING BLOCK FOR



kments,"  
ent Dams  
ng'g, San  
Dynamic  
7. July,  
s," Proc.  
3, Purdue  
the San  
h. Eng'g,  
is of the  
9, 1971,"  
Induced  
Berkeley,  
s," Ph.D.  
hquake-  
4, Dec.,  
mic Risk  
l Eng'g.

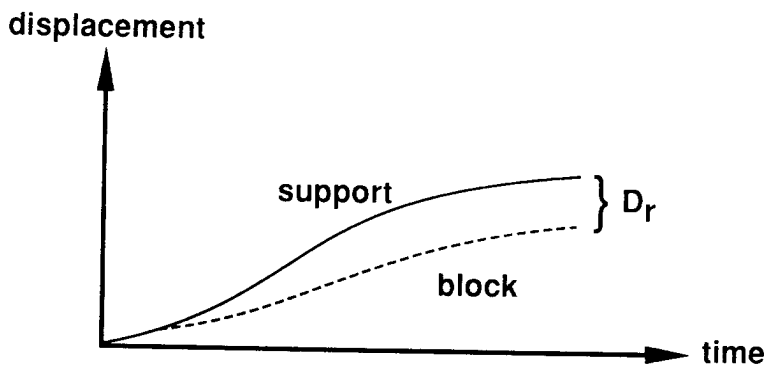
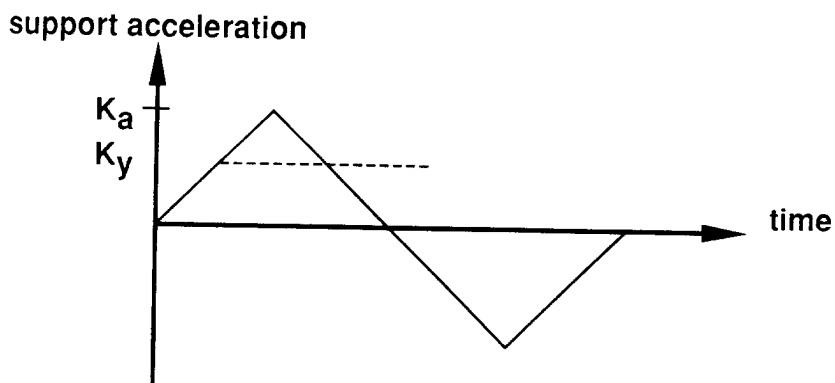
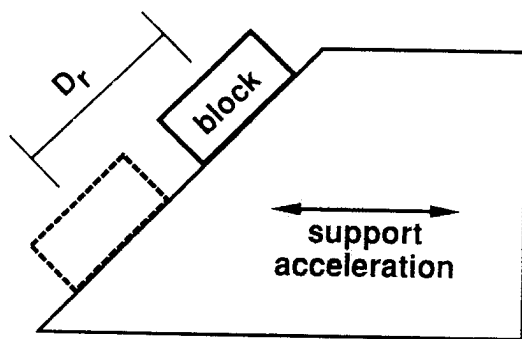


FIGURE 1 SLIDING BLOCK REPRESENTATION OF RELATIVE DISPLACEMENT FOR TRIANGULAR BASE EXCITATION

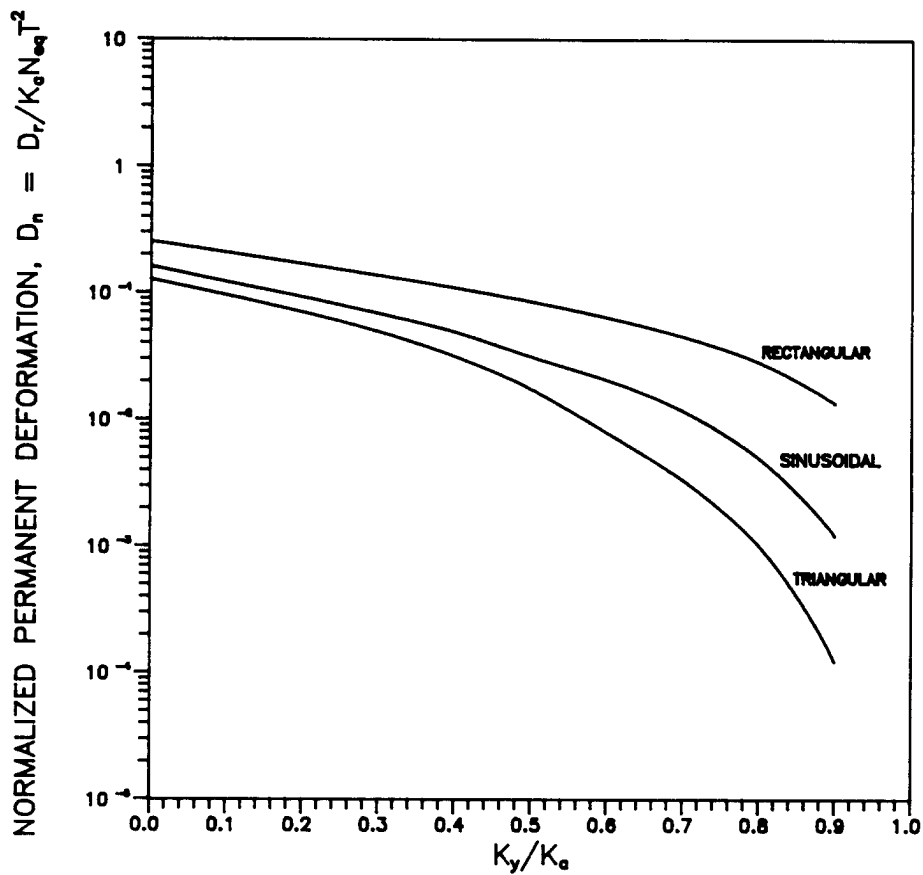


FIGURE 2 NORMALIZED PERMANENT DEFORMATION VS.  $K_y / K_a$  FOR 3 SIMPLE BASE MOTIONS CONSIDERED

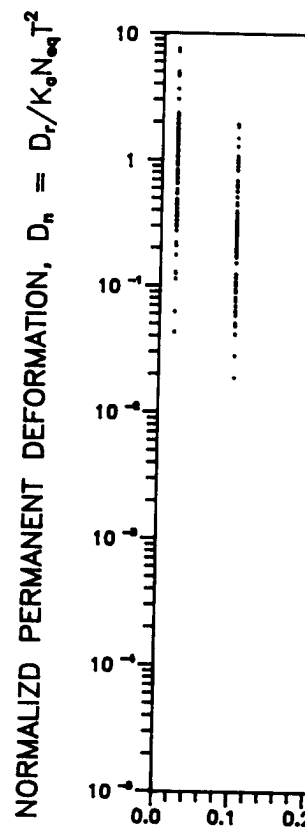


FIGURE 3 NORM  
86 (

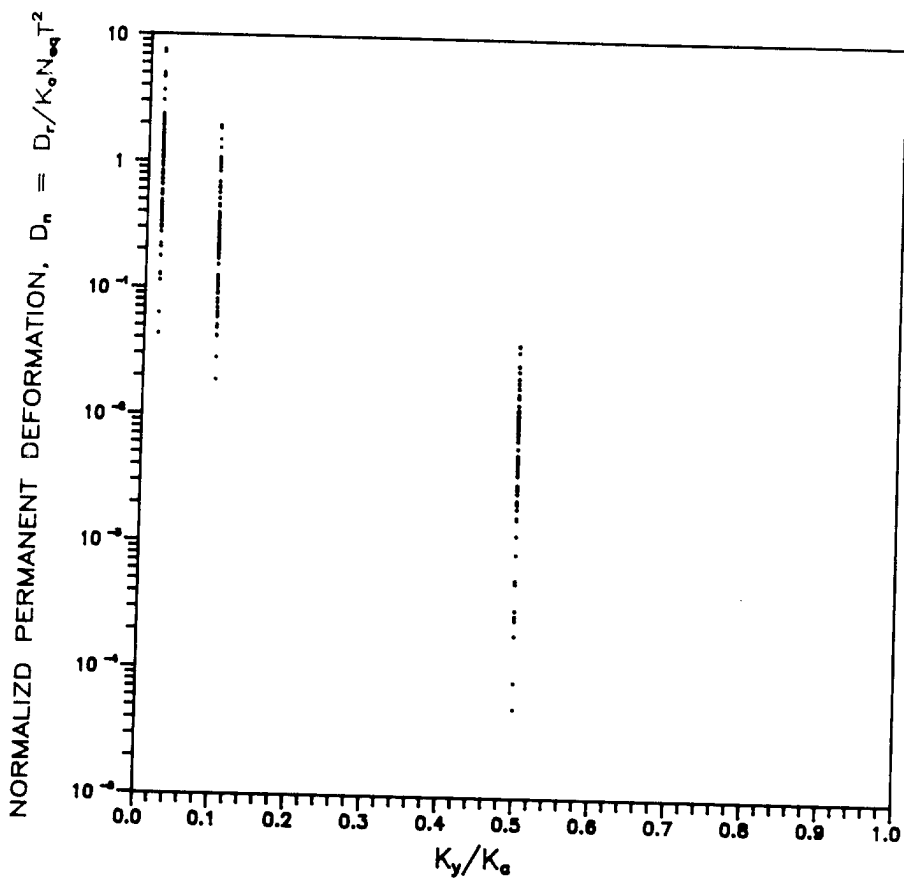


FIGURE 3 NORMALIZED PERMANENT DEFORMATIONS FROM 86 GROUND MOTION RECORDS VS.  $K_y/K_0$

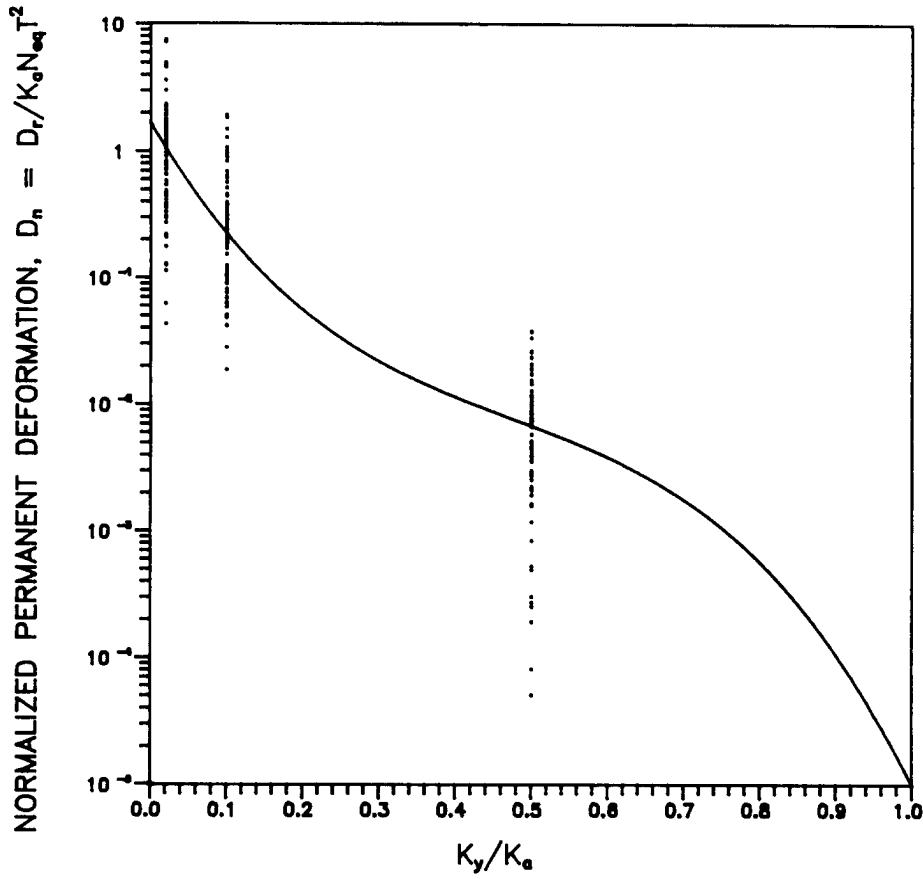


FIGURE 4 FUNCTION FOR NORMALIZED PERMANENT DEFORMATION BASED ON ACTUAL EARTHQUAKE RECORDS

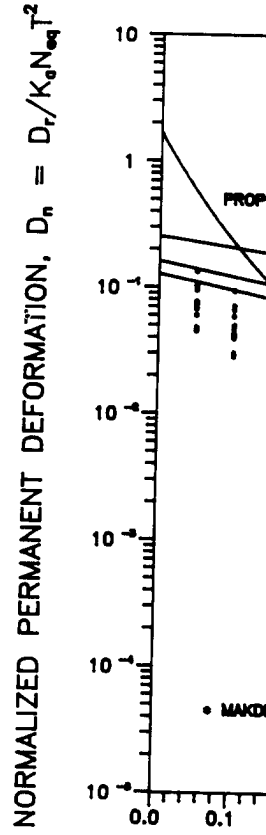


FIGURE 5 NORMALIZED PERMANENT DEFORMATION (COMPARISON OF PROPOSED MODEL AND MAKDISI MODEL)

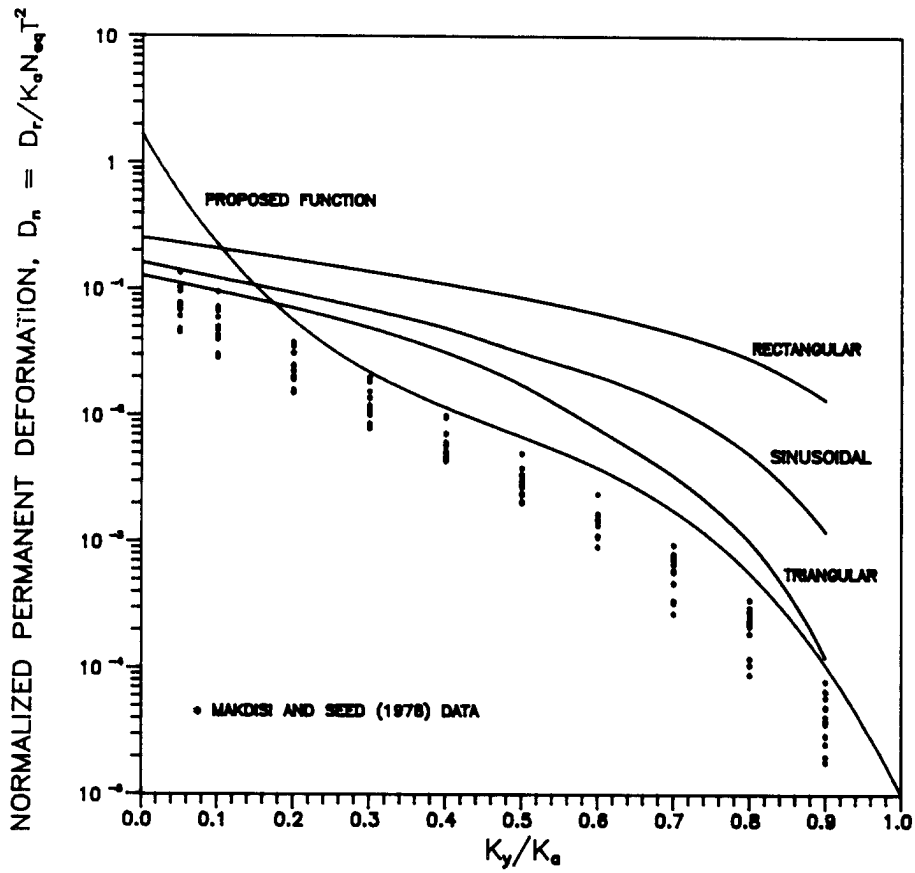


FIGURE 5 NORMALIZED PERMANENT DEFORMATION VS.  $K_y / K_a$   
 (COMPARISON OF THE PROPOSED DEFORMATION FUNCTION  
 MAKDISI AND SEED DATA AND 3 SIMPLE BASE MOTIONS)